Quadratic Hawkes processes for financial prices - Pierre Blanc, Jonathan Donier, Jean-Philippe Bouchaud

Benjamin Cohen

April 12, 2024

Abstract

This paper introduces and explores the main characteristics of the QHawkes model, an extension of the Hawkes [Haw71] price model by incorporating linear and quadratic feedback effects in the jump intensity based on past returns. Empirical analysis of NYSE stock data reveals structural differences in the off-diagonal component of the quadratic kernel compared to standard Hawkes models [HJR15]. The QHawkes model demonstrates two key properties essential for modeling volatility processes: time-reversal asymmetry similar to financial markets and the generation of fat-tailed volatility processes, particularly under exponentially decaying kernels, with connections to Pearson diffusions [Pea48] in the continuous limit [FS16]. The paper discusses various properties of QHawkes processes, including their ability to generate long memory without being at the critical point. Numerical simulations of the calibrated QHawkes model confirm its capability to replicate fat-tails and time reversal asymmetry observed in empirical time series with minimal quadratic non-linearity.

Contents

1 Introduction: Fractional Brownian Motions, GARCH Models, and Hawkes Processes

The quest for an ideal statistical model of financial markets continues since the inception of the Brownian motion model by Bachelier. Numerous mathematical frameworks have been proposed to capture essential stylized facts of financial time series, such as fat-tailed return distributions and volatility clustering. Notable among these are GARCH-like models and stochastic volatility models, although they have limitations in terms of conditional Gaussianity of returns and lack of deeper theoretical underpinnings.

Another crucial aspect often overlooked is the time-reversal asymmetry (TRA) of financial time series, characterized by past and future interchanges not being statistically symmetrical. Two distinct effects break this symmetry: the leverage effect and the Zumbach effect [Zum08, PHPS10]. While continuous-time stochastic volatility models adhere to time-reversal symmetry (TRS), GARCH-like models exhibit TRA, albeit stronger than observed in empirical data.

Hawkes processes, initially developed in earthquake statistics, offer a middle ground between purely stochastic and agent-based models in finance. These processes model the activity rate at time t, λ_t, as dependent on the history of the point process itself via an auto-regressive relation:

$$\lambda_t = \lambda_\infty + \int_{-\infty}^{t} \phi(t-s) dN_s,$$

where λ_∞ is a baseline intensity and ϕ is a non-negative, measurable function satisfying $\|\phi\|_1 = \int_0^\infty \phi(s)ds \leq 1$. Despite their success in capturing certain features of financial data, Hawkes processes cannot account for TRA observed in empirical time series.

Motivated by these shortcomings, this paper proposes QHawkes models, which extend the Hawkes formalism to include features of QARCH models [BILL17]. The inclusion of feedback from actual price changes into market activity aims to address deficiencies in capturing fat tails in return distributions and TRA. The paper outlines the general model, explores its core properties, introduces a sub-family termed ZHawkes capturing TRA, and calibrates the model on intra-day US stock data. Additionally, the paper discusses the Markovian nature of the process in the case of exponential kernels and provides numerical simulations confirming its ability to replicate empirical TRA and fat-tailed volatility.

2 The Quadratic-Hawkes Model

2.1 Overview

The QHawkes (Quadratic Hawkes) process (P_t), $t \geq 0$, is akin to Hawkes processes, constituting a self-exciting point process where the intensity λ_t hinges on past occurrences within the process. Named for its quadratic nature regarding $dP_{s<t}$, the model represents the intensity of price shifts via the equation:

$$\lambda_t = \lambda_\infty + \frac{1}{\psi}\int_{-\infty}^{t} L(t-s)dP_s + \frac{1}{\psi^2}\int_{-\infty}^{t}\int_{-\infty}^{t} K(t-s, t-u)dP_s dP_u,$$

Here, P denotes high-frequency prices, modeled as a pure jump process with signed increments. The kernel $L : \mathbb{R}^+ \to \mathbb{R}$ reflects linear coupling between price changes and market activity, while $K : \mathbb{R}^+ \times \mathbb{R}^+ \to \mathbb{R}$ signifies a quadratic feedback kernel. λ_∞ represents the baseline intensity in the absence of feedback. This formulation represents an expansion of price change intensity concerning past prices, truncated to the second order.

While acknowledging the importance of leverage on daily scales, the insignificance of L on intra-day scales allows focusing solely on the quadratic kernel:

$$\lambda_t = \lambda_\infty + \frac{1}{\psi^2}\int_{-\infty}^{t}\int_{-\infty}^{t} K(t-s, t-u)dP_s dP_u.$$

This model serves as a generalization of the Hawkes process for prices, simplifying to a Hawkes process when certain conditions are met.

The linear Hawkes process exhibits a branching structure, where each event triggers a Poisson-distributed set of subsequent events. The parameter $n_H = ||\phi||_1$ quantifies the endogeneity, indicating

the fraction of internally triggered events. This intuition extends to the QHawkes model, where event rates depend on interactions between pairs of events. Positive feedback in $K(s,t) \geq 0$ amplifies future volatility when events align in direction, while compensatory events inhibit volatility, aligning with empirical observations.

2.2 Special Case: The ZHawkes Model

The ZHawkes model, tailored from QHawkes, eliminates leverage and structures the quadratic feedback kernel K:

$$K(t,s) = \phi(t)\delta_{t-s} + k(t)k(s),$$

where ϕ and k are positive functions. This simplifies λ_t to $\lambda_\infty + H_t + Z_t^2$, where the "Hawkes term" is given by:

$$H_t := \int_{-\infty}^{t} \phi(t-s)dN_s; \quad N_t - N_{t^-} := \frac{1}{\psi^2}(P_t - P_{t^-})^2$$

and the "Zumbach term" is given by:

$$Z_t = \frac{1}{\psi}\int_{-\infty}^{t} k(t-s)dP_s$$

2.3 Mathematical Formulation

The components include the pure jump process P_t, intensity (λ_t), punctual Poisson measure $m(dt, d\xi)$, and kernels K and L. The quadratic kernel $K : \mathbb{R}^+ \times \mathbb{R}^+ \to \mathbb{R}$ satisfies:

- Symmetry: $\forall s,t \geq 0$, $K(t,s) = K(s,t)$.
- Positivity: $\forall f \in L^2(\mathbb{R}^+)$, $\iint_{\mathbb{R}^+\times\mathbb{R}^+} K(t,s)f(t)f(s)\,dt\,ds \geq 0$.
- Non-explosion: $\int_0^\infty |K(t,t)|\,dt < +\infty$.

The operator Tr(K) is defined as the trace of the kernel K, and it maps functions from $L^2(\mathbb{R}^+)$ to itself. This operator sums the diagonal elements of K and ensures that the integral of K(t,t) over all t in R^+ is finite.

$$\mathrm{Tr}(K) = \int_0^\infty K(t,t)\,dt < +\infty \tag{1}$$

Additionally, it verifies that $K(t,t) \geq 0$ for all $t \geq 0$. L is the leverage kernel function from $\mathbb{R}^+$ to $\mathbb{R}$ assumed measurable. Analogous to QARCH models, it should be dominated by K for positivity of the intensity λ_t. However, given its minimal effect observed in subsequent analysis, we defer further investigation of this positivity condition to future research.

2.4 Required Criterion for Time Stationarity

The stationarity condition is satisfied when either $\lambda_\infty > 0$ and $\mathrm{Tr}(K) < 1$, or when $\lambda_\infty = 0$ and $\mathrm{Tr}(K) = 1$. Specifically, for the ZHawkes process, the endogeneity ratio is given by:

$$\mathrm{Tr}(K) = ||\phi||_1 + ||k^2||_1 \equiv n_H + n_Z,$$

where n_H represents the standard "Hawkes norm" and $n_Z \equiv ||k^2||_1$ denotes the "Zumbach norm".

2.5 Autocorrelation Structure and Asymptotic Trends

Assumption: No leverage, L = 0. Exact equations relate auto-correlation functions (C, D) to kernel K, enabling inference from observed data. The auto-correlation function $C(\tau)$ and the three-point correlation function $D(\tau_1, \tau_2)$ are defined as:

$$C(\tau) = E\left[\frac{dN_t}{dt}\frac{dN_{t-\tau}}{dt}\right] - \lambda^2, \quad D(\tau_1,\tau_2) = \frac{1}{\psi^2}E\left[\frac{dN_t}{dt}\frac{dP_{t-\tau_1}}{dt}\frac{dP_{t-\tau_2}}{dt}\right].$$

In the asymptotic behavior analysis, assuming power-law decays for the kernel and auto-correlation functions, we have when $\tau \to \infty$:

$$\begin{cases} K(\tau,\tau) \sim c_0 \tau^{-1-\epsilon} & \text{(diagonal, } \epsilon > 0\text{)} \\ K(\tau v_1, \tau v_2) \sim \tilde{K}(v_1,v_2)\tau^{-2\delta} & \text{(off-diagonal, } \delta > \frac{1}{2}\text{)} \\ C(\tau) \sim c_1 \tau^{-\beta} & \text{(2-points AC)} \\ D(\tau,\tau) \sim c_2 \tau^{-\beta_0} & \text{(3-points AC, diagonal)} \\ D(\tau v_1, \tau v_2) \sim \tilde{D}(v_1,v_2)\tau^{-2\rho} & \text{(3-points AC, off-diagonal)} \end{cases}$$

c_0, c_1, c_2 constants. $\tilde{K}(v_1,v_2)$, $\tilde{D}(v_1,v_2)$ bounded functions of (v_1,v_2). $||\phi||_1 < \infty \implies \epsilon > 0$ and $\delta > \frac{1}{2} \implies$ second and third moments finite. Assuming $\epsilon < 1$ leads to $K(\tau_1,\tau_2) \sim \tau_1^{-1-\epsilon}$ narrow around diagonal $|\tau_1 - \tau_2| \ll \tau_1, \tau_2$, off-diagonal: power-law.

$$\text{For } Tr(K) < 1 : \begin{cases} \delta > \frac{3+\epsilon}{4} & \Rightarrow \beta = 1+\epsilon, \beta_0 = 1+\epsilon, \rho = \delta \\ \frac{2+\epsilon}{3} < \delta < \frac{3+\epsilon}{4} & \Rightarrow \beta = 4\delta - 2, \beta_0 = 1+\epsilon, \rho = \delta \\ 2 < \delta < \frac{2+\epsilon}{3} & \Rightarrow \beta = 4\delta - 2, \beta_0 = 3\delta - 1, \rho = \delta \end{cases}$$

In this non-critical scenario, the interpretation is straightforward. For instance, in the first phase, the auto-correlation is directly influenced by the diagonal part of the kernel, while in the last two phases, off-diagonal effects generate correlations with slower decay, potentially leading to long-memory processes when $\frac{1}{2} < \delta < \frac{3}{4}$.

$$\text{For } Tr(K) \to 1, \lambda_\infty \to 0 : \begin{cases} \delta > \frac{3}{4} & \Rightarrow \beta = 1-2\epsilon, \beta_0 = 1-\epsilon, \rho = \delta \\ \frac{2}{3} < \delta < \frac{3}{4} & \Rightarrow \beta = 4\delta - 2\epsilon - 2, \beta_0 = 1-\epsilon, \rho = \delta \\ \frac{1+\epsilon}{2} < \delta < \frac{2}{3} & \Rightarrow \beta = 4\delta - 2\epsilon - 2, \beta_0 = 3\delta - \epsilon - 1, \rho = \delta \end{cases}$$

In the critical case, the relation between parameters changes, requiring $0 < \epsilon < \frac{1}{2}$ for the process to exist. This critical process always exhibits long-memory behavior ($\beta < 1$) or becomes trivial otherwise, similar to the linear Hawkes process.

3 The Intra-day Quadratic-Hawkes Model

3.1 Quadratic-Hawkes as as a limit of QARCH

Now, let's delve into the relationship between the QHawkes and discrete QARCH models. This exploration will offer a method to calibrate QHawkes using discretely sampled price time series. For a constant time step $\Delta > 0$, we define for all $t \in \mathbb{R}$:

- Price increment $[t, t+\Delta]$: $r_t^\Delta = P_{t+\Delta} - P_t$
- Volatility in t: $\sigma_t^\Delta = \sqrt{\mathbb{E}\left[(r_t^\Delta)^2 \,|\, \mathcal{F}_t\right]}$

QHawkes: limit when $\Delta \to 0^+$ of QARCH.

$$(\sigma_t^\Delta)^2 = (\sigma_\infty^\Delta)^2 + \sum_{\tau \geq 1} L^\Delta(\tau) r_{t-\tau\Delta}^\Delta + \sum_{\tau,\tau_0 \geq 1} K^\Delta(\tau,\tau_0) r_{t-\tau\Delta}^\Delta r_{t-\tau_0\Delta}^\Delta$$

where $(\sigma_\infty^\Delta)^2 = \psi^2 \lambda_\infty \Delta$, $L^\Delta(\tau) = L(\tau\Delta)\Delta$, and $K^\Delta(\tau,\tau_0) = K(\tau\Delta, \tau_0\Delta)\Delta$. Indeed, for $t \in \mathbb{R}$,

$$\mathbb{E}[(r_t^\Delta)^2 | F_t] = \psi^2 \mathbb{P}(P_{t+\Delta} - P_t \neq 0 | F_t) + o(\Delta) \quad = \psi^2 \lambda_t \Delta + o(\Delta)$$

$$\frac{(\sigma_t^\Delta)^2}{\Delta} \xrightarrow{\Delta \to 0^+} \psi^2 \lambda_t$$

Connection between models allows for calibrating a QARCH model on intraday 5-minute bin returns providing insights into the underlying QHawkes model's structure. Directly calibrating the QHawkes model is more challenging due to increased noise and computational demands.

3.2 Intra-day Calibration of a QARCH Model

3.2.1 Dataset and Notations

The dataset spans from January 1, 2000, to December 31, 2009, containing data for 133 NYSE stocks across 2499 trading days, each segmented into 78 five-minute bins. Within each bin, open, close, high, and low prices ($O, C, H, L > 0$) are recorded. We employ logarithmic transformations to define:

- Return: $r = \ln(C/O)$
- Rogers-Satchell volatility: $\sigma^{RS} = \sqrt{\ln(H/O) \times \ln(H/C) + \ln(L/O) \times \ln(L/C)}$

3.2.2 Normalization Procedure

Normalize the dataset by treating intra-day prices as independent realizations of a stationary stochastic process. This entails calculating the cross-sectional intra-day volatility pattern for each trading day to standardize the data for each stock. By doing so, collective shocks on a given day are mitigated, providing a clearer understanding of individual stock behavior. Additionally, leverage both intra-day and overnight volatility to eliminate daily feedback effects, allowing for a more focused analysis on the pure intra-day dynamics, devoid of external influences.

- Calculate the cross-sectional volatility pattern for each trading day.
- Normalize the returns and Rogers-Satchell volatility using the open-to-close volatility and cross-sectional intra-day pattern.
- Exclude trading days with exceptional returns exceeding six standard deviations from the mean.
- Ensure uniformity across the stock market by standardizing the mean of the squares to one and adjusting the average return to zero.

3.2.3 Calibration Results

Initial Estimation of Kernels: Initially, kernels are estimated using the Generalized Method of Moments (GMM), followed by Maximum Likelihood Estimation (MLE) with t-distributed residuals to accommodate fat tails.

- **Off-Diagonal Structure:** The feedback matrix exhibits an off-diagonal structure.
- **Intra-Day Leverage Kernel:** The intra-day leverage kernel is nearly zero, justifying $L \equiv 0$.
- **Spectral Decomposition:** Analysis of the quadratic kernel's spectral decomposition reveals it as a composite of a positive rank-one matrix and a diagonal one. The kernel can be approximated as $K(\tau, \tau_0) \approx \phi(\tau)\delta_{\tau-\tau_0} + k(\tau)k(\tau_0)$, with $\phi(\tau) = g\tau^{-\alpha}$ and $k(\tau) = k_0 \exp(-\omega\tau)$, where $g = 0.09$, $\alpha = 0.60$, $k_0 = 0.14$, and $\omega = 0.15$.
- **Modeling Residuals:** Residuals are fit with a Student's t-distribution, resulting in $\nu \approx 7.9$ degrees of freedom and a kurtosis $\kappa \approx 4.5$, explaining the fat tails of five-minute returns due to quadratic feedback.
- **Endogeneity Ratio:** The endogenous ratio of volatility, represented by the trace of the quadratic kernel, is approximately 80%, indicating that 80‘% of intra-day volatility stems from endogenous feedback effects.

Kernel Calibration: The off-diagonal part of the kernel K is set to its fitted value $K(\tau, \tau_0) = k(\tau)k(\tau_0) = k_0^2 \exp(-\omega(\tau + \tau_0))$, while the diagonal is recalibrated with a longer maximum lag of 60 bins (equivalent to five hours of trading). This recalibration yields $\phi(\tau) = g_0\tau^{-\alpha_0}$ with updated coefficients $g_0 = 0.09$ and $\alpha_0 = 0.76$, similar to those obtained over a shorter time span.

Modeling Residuals: Residuals ξ_t of the QARCH model, defined by $r_t = \sigma_t\xi_t$, are modeled using Student's t-distribution. The calibration of the model with $K(\tau, \tau_0) = \phi(\tau)\delta_{\tau-\tau_0} + k(\tau)k(\tau_0)$ yields $\nu \approx 7.9$ degrees of freedom for the residuals, resulting in a kurtosis $\kappa \approx 4.5$. This suggests that

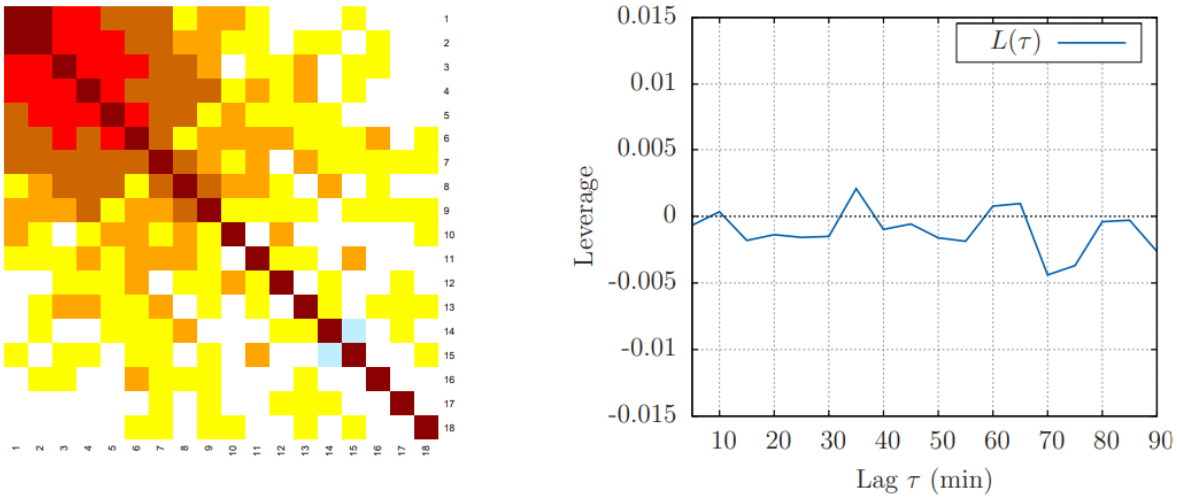

Figure 1: Visualization of Quadratic and Leverage Kernels.
Left: Heatmap of the quadratic kernel. Right: Leverage kernel display.

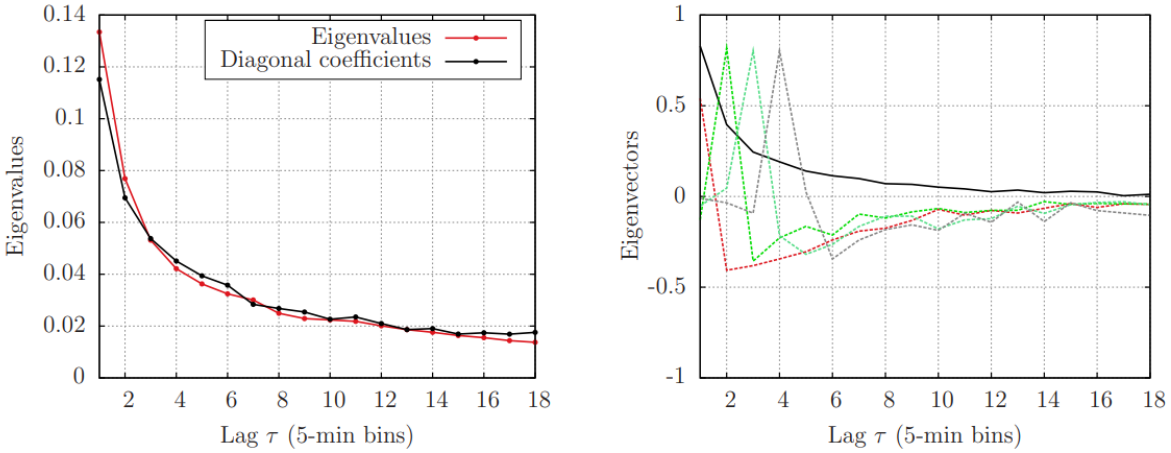

Figure 2: Analysis of Ranked Eigenvalues and Corresponding Eigenvectors.
Left: Ranked eigenvalues. Right: Eigenvectors corresponding to the five largest eigenvalues.

the QARCH model adequately captures the fat tails of five-minute returns, primarily induced by the quadratic feedback mechanism.

Endogeneity Ratio: In the QARCH model, the endogeneity ratio of volatility is determined by the trace $\mathrm{Tr}(K)$ of the quadratic kernel. With a maximum lag of $q \geq 1$, this ratio is calculated as $\mathrm{Tr}(K) = \sum_{\tau=1}^{q} \phi(\tau) + \sum_{\tau=1}^{q} k^2(\tau)$. Utilizing fits for $k(\tau)$ and $\phi(\tau)$, $\mathrm{Tr}(K)$ for $q = 78$ is approximately 0.80, indicating that 80% of intra-day volatility is attributable to endogenous feedback effects.

Figures Overview: Several figures provide visual representations. Figure 1 shows calibrated QARCH kernels based on five-minute intra-day returns for US stocks. Figure 2 presents the spectral decomposition of the quadratic QARCH kernel. Figure 3 illustrates the fit of the kernel K by a combination of power-law and exponential components. Figure 4 displays the long-range kernel heatmap, with off-diagonal elements constrained to an exponential rank-one fit and diagonal elements adjusted freely. Additionally, it presents the Hawkes kernel $\phi(\tau)$ fitted using 60 bins, plotted in log-log scale with a dashed line indicating a power-law fit with exponent $\alpha_0 = 0.76$.

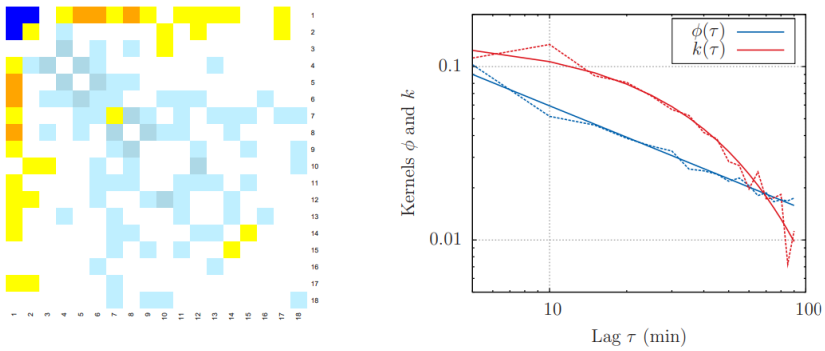

Figure 3: Fit of Kernel K with Power-Law and Exponential Components. Left: Illustration of the difference between the fitted and original matrices, highlighting stronger short-term feedback in the upper-left corner. Right: Kernels $\phi(\tau)$ and $k(\tau)$ minimizing matrix distance, plotted in log-log scale. The rank-one kernel k (red) dominates for small τ, while the diagonal kernel ϕ (blue) follows a power-law ($\alpha = 0.6$) and an exponential fit with a characteristic time of about 30 minutes.

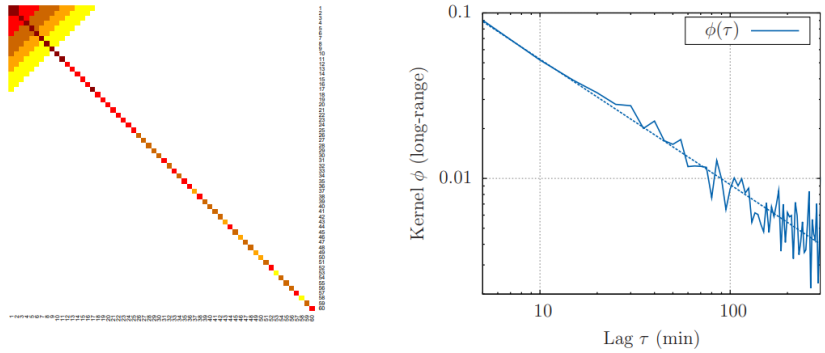

Figure 4: Representation of Long-Range Kernel and Hawkes Kernel. Left: Heatmap of the long-range kernel, with the off-diagonal fixed as its exponential rank-one fit, and with the diagonal calibrated without constraints. Right: Plot of the Hawkes kernel $\phi(\tau) = K(\tau, \tau) - k^2(\tau)$ fitted using 60 bins. The kernel $\phi(\tau)$ is presented in log-log scale, with its power-law fit having an exponent $\alpha_0 = 0.76$ (indicated by the dashed line).

4 Analysis of Volatility in the ZHawkes Model

4.1 Model Dynamics with Exponential Kernels

When the kernels $\phi(\cdot)$ and $k(\cdot)$ in the ZHawkes model take on exponential forms, the model's behavior becomes Markovian, enabling its evolution to be characterized by a stochastic differential equation. Assuming binary price jumps, $\xi = \pm\psi$, with $\psi = 1$, and define $k(t) = \sqrt{2n_Z\omega}\exp(-\omega t)$ and $\phi(t) = n_H\beta\exp(-\beta t)$, where n_H and n_Z represent the Hawkes and Zumbach norms, respectively.
$\mathrm{Tr}(K) = n_H + n_Z < 1 \implies \lambda_t = \lambda_\infty + H_t + Z_t^2$, with:

$$dH_t = \beta[-H_t dt + n_H dN_t],$$
$$dZ_t = -\omega Z_t dt + k_0 dP_t.$$

N and P jump simultaneously with intensity λ_t and amplitudes $\Delta N_\tau = 1$, $\Delta P_\tau = \pm 1$.

4.2 Low-frequency asymptotics

Here we delve into the low-frequency behavior of nearly critical Hawkes processes with short-ranged kernels. By scaling appropriately and approaching the critical point where $n_H = 1$, the short-memory Hawkes-based price process converges to a Heston process, as the Hawkes intensity converges to a CIR volatility process.

When the kernel follows a power-law behavior $\phi(t) \sim t^{-1-\varepsilon}$ with $1/2 < \varepsilon < 1$, the limiting process for the intensity becomes a fractional Brownian motion with Hurst exponent $H = \varepsilon - \frac{1}{2}$. For ε close to $1/2$, as observed in empirical data, the roughness of this process aligns with a Hurst exponent H close to zero for the log-volatility ($H = 0$ for the multifractal model). However, the connection between the Hawkes process intensity and the log-volatility remains unclear. A fat-tailed behavior, which is absent in simple linear Hawkes processes and Heston-CIR processes, cannot be reproduced.

Now, let's delve into the low-frequency asymptotics of the Markovian ZHawkes model. Study of scaling behavior by defining processes $\overline{H}_t^T = H_{tT}$, $\overline{Z}_t^T = Z_{tT}$, $\overline{N}_t^T = N_{tT}$, and $\overline{P}_t^T = P_{tT}$, with β^T and ω^T as parameters that may depend on T, but with fixed endogeneity parameters n_H and n_Z.

$$\begin{cases} d\overline{H_t}^T &= -\beta_T[\overline{H_t}^T T dt + n_H d\overline{N_t}^T] \\ d\overline{Z_t}^T &= -\omega_T \overline{Z_t}^T T dt + \gamma^T d\overline{P_t}^T \end{cases} \tag{2}$$

Scaling $\beta^T = \frac{\beta}{T}$ and $\omega^T = \frac{\omega}{T}$, the infinitesimal generator of the process becomes:

$A^T f(h,z) = -\beta h \frac{\partial f}{\partial h}(h,z) - \omega z \frac{\partial f}{\partial z}(h,z) + \frac{T^2}{2}\left(\lambda_\infty + h + z^2\right)\left[f\left(h + n_H \beta T, z + \gamma\sqrt{T}\right) + f\left(h + n_H \beta T, z - \gamma\sqrt{T}\right) - f(h,z)\right]$

$A^T f(h,z)$ converges to

$A^\infty f(h,z) = -\beta[(1-n_H)h - n_H(\lambda_\infty + z^2)]\frac{\partial f}{\partial h}(h,z) - \omega z \frac{\partial f}{\partial z}(h,z) + n_Z \omega(\lambda_\infty + h + z^2)\frac{\partial^2 f}{\partial z^2}(h,z)$

The operator A^∞ is the infinitesimal generator of the diffusion:

$$\begin{cases} d\overline{H}_t^\infty &= [-(1-n_H)\overline{H}_t^\infty + n_H\left(\lambda_\infty + (\overline{Z}_t^\infty)^2\right)]\beta dt, \\ d\overline{Z}_t^\infty &= -\omega \overline{Z}_t^\infty dt + \gamma\sqrt{\lambda_\infty + \overline{H}_t^\infty + (\overline{Z}_t^\infty)^2}\, dW_t \end{cases}$$

where W is a standard Brownian motion. This implies convergence of the process $(\overline{H}^T, \overline{Z}^T)$ to $(\overline{H}^\infty, \overline{Z}^\infty)$ as T goes to infinity. Thus, the norm of the process need not tend to 1 for a non-degenerate limit process to be obtained. The limiting process A^∞ is the primary focus of this section.

As T goes to infinity, the process $(\overline{H}^T, \overline{Z}^T)$ converges to $(\overline{H}^\infty, \overline{Z}^\infty)$. Thus, a non-degenerate limit process can be obtained without the need for the process's norm to tend to 1 (i.e., the process being nearly critical). This limiting process is a significant result, believed to apply to the entire class of non-critical ZHawkes processes with short memory. The limiting behavior corresponding to long-memory/critical ZHawkes processes is a subject for future investigations.

4.3 Tail of the Volatility Distribution

We are studying the limiting process of $\overline{H}$ and $\overline{Z}$. We find that the SDE for $\overline{H}$ allows for an explicit solution, while the SDE for $\overline{Z}$ becomes an autonomous, non-Markovian equation. First, we examine the scenario without Hawkes feedback ($n_H = 0$), where only the Zumbach term is present. This model still captures key empirical properties of volatility. We derive the stationary density of the process V, which exhibits a power-law tail, depending solely on the Zumbach norm n_Z. In the case with Hawkes feedback ($n_H > 0$), the tail exponent of the activity distribution can still be analytically computed in certain limits, indicating how both the Hawkes and Zumbach feedback mechanisms contribute to fat-tailed volatility distributions. These findings shed light on the dynamics of financial markets and highlight the need for mechanisms to explain the observed universality of tail exponents.

5 Numerical simulation results

5.1 Empirical tails of the volatility process

Comparison of the ZHawkes, standard Hawkes-based price and financial data volatility processes. Simulation of ZHawkes with exponential Zumbach part and power-law Hawkes, using parameters inspired by the QARCH calibration.

$$\phi(t) = 0.0016 \times (1 + 0.01 \times t)^{-1.2} \tag{3}$$

$$k(t) = 0.003 \times \exp(-0.03 \times t) \tag{4}$$

with resulting $n_H = 0.8$, $n_Z = 0.1$, and $Tr(K) = 0.9$.
Benchmark: standard Hawkes-based price process ($n_Z \equiv 0$) with:

$$\phi = (1 + 0.01 \times t)^{-1.3}, \quad n_H = 0.99 \tag{5}$$

To estimate the empirical tail exponent of the volatility, Hill [Hil84] exponent:

$$\nu_{hill} = 1 + \frac{1}{\frac{1}{n}\sum_{i=1}^{n} \log\left(\frac{\sigma_i}{\sigma_{\min}}\right)} \tag{6}$$

We obtain $\nu_{hill} = 4.50$ for the (normalized) five-minute returns of US stocks, $\nu_{hill} = 5.07$ for the ZHawkes, and $\nu_{hill} = 12.4$ for the standard Hawkes-based without ZHawkes feedback.

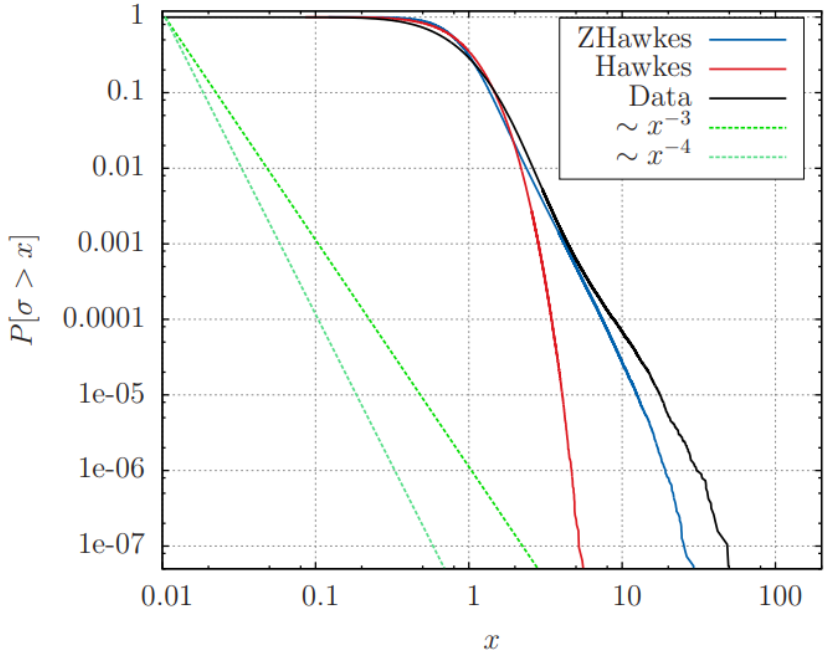

Figure 5: Cumulative density function of the Rogers-Satchell volatility for US stock data (plain line), simulated Hawkes data (red dashed line), and simulated ZHawkes data (blue dot-dashed line).

Despite a close-to-one norm and a slowly-decaying kernel, the standard Hawkes model can't replicate the observed tails in US stock data. In contrast, the ZHawkes model, with a norm below unity and a short-lived Zumbach effect, naturally generates similar fat tails, even with a relatively small n_Z.

5.2 Time-Reversal Asymmetry (TRA)

We also examine the time-reversal asymmetry (TRA) of price time series. We measure the amount of TRA for the simulated ZHawkes process, the Hawkes benchmark, and the financial dataset studied earlier.

We consider returns and Rogers-Satchell volatilities defined for intraday five-minute bins, with a fixed maximum lag $q = 36$ (equivalent to 3 hours of trading). We introduce the time asymmetry ratios $\Delta(\tau)$ using:

$$C(\tau) = \frac{< \sigma_t^{RS} \times |r_{t-\tau}| > - < \sigma^{RS} >< |r| >}{\sqrt{< \sigma^{RS^2} > - < \sigma^{RS} >^2}\sqrt{< r >^2 - < |r| >^2}} \tag{7}$$

$$\Delta(\tau) = \frac{\sum_{\tau'=1}^{q}[C(\tau') - C(-\tau')]}{2\sum_{\tau'=1}^{q} \max(|C(\tau')|, |C(-\tau')|)} \tag{8}$$

We compare these ratios for real stock returns, returns simulated with the ZHawkes model, and returns simulated with a standard Hawkes-based price model. Absolute returns instead of squared returns for computing the cross-correlation function, as it provides more stable and less noisy results, particularly in the presence of tail events.

While standard Hawkes shows negligible time-reversal asymmetry (TRA), failing to capture the observed asymmetry in intra-day volatility, the ZHawkes model exhibits some asymmetry, albeit with a concave $\tau \mapsto \Delta(\tau)$ function. Real data, however, surprisingly shows convexity, possibly due to non-stationarity not captured by simple models.

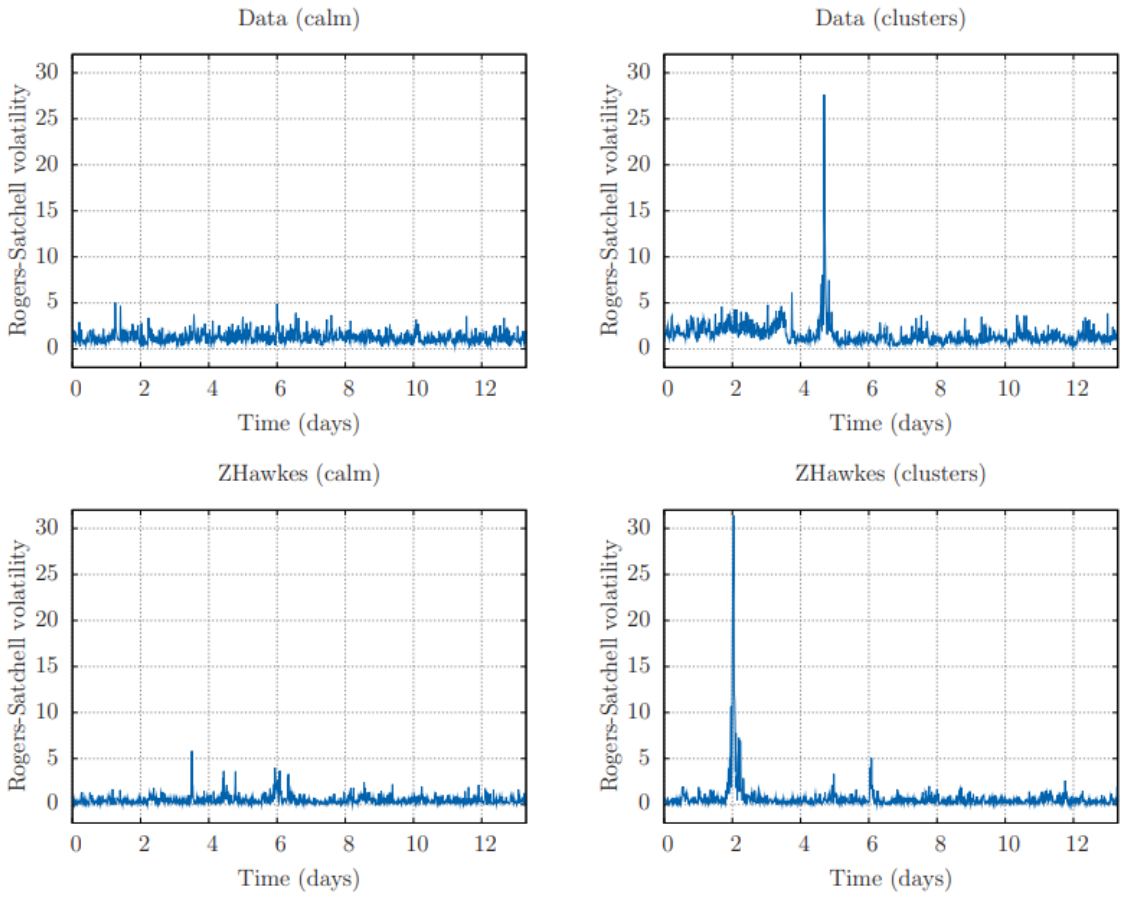

Figure 6: Time series of Rogers-Satchell volatility. Left: period of calm ; Right: cluster of intense activity.

6 Conclusion

The study underscores that the traditional Hawkes feedback mechanism fails to capture crucial dynamics of markets, such as fat-tailed volatility and time-reversal asymmetry. To address this, we introduce QHawkes processes, extending Hawkes models to incorporate feedback not only on past activity but also on past price returns. Calibration of QHawkes on intraday returns of NYSE stocks reveals compelling properties, including multiplicative volatility dynamics and the reproduction of observed time asymmetry in financial data.

ZHawkes, a component of QHawkes, exhibits intriguing features absent in standard Hawkes processes, such as generating power-law tails in volatility and returns and potentially displaying long memory. The continuous limit equations for QHawkes resemble tractable generalizations of Pearson diffusions, aligning well with empirical findings. Further exploration of QHawkes models promises valuable insights into market dynamics, with implications for market design and understanding volatility processes from micro to macro scales.

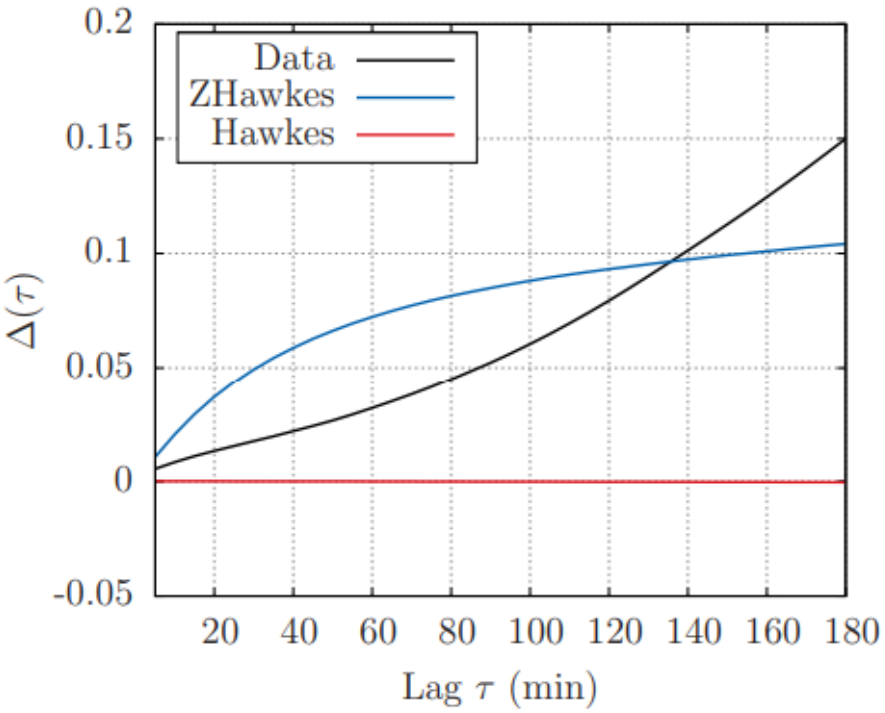

Figure 7: Time asymmetry ratio $\Delta(\tau)$ for US stock data (plain line), simulated Hawkes model (red line), and simulated ZHawkes model (blue dot-dashed line). Note that the Hawkes process does not generate any detectable TRA.

7 Personal Reflections

7.1 Positive Critiques

The analysis presented in the preceding sections offers valuable insights into the dynamics of intra-day volatility and the role of feedback mechanisms in the QARCH model. The calibration results provide a comprehensive understanding of the intricate relationships between different components of the model and empirical observations. The identification of off-diagonal structures in the feedback matrix and the characterization of intra-day leverage kernels contribute significantly to the understanding of market dynamics. Furthermore, the modeling of residuals with Student's t-distribution and the estimation of the endogeneity ratio of volatility offer novel perspectives on volatility modeling. The paper introduces and explores the main characteristics of QHawkes models, providing insights into the dynamics of intra-day volatility and the role of feedback mechanisms in the jump intensity based on past returns. The empirical analysis on NYSE stock data reveals structural differences in the off-diagonal component of the quadratic kernel compared to standard Hawkes models, enriching our understanding of market microstructure. The demonstration of time-reversal asymmetry similar to financial markets and the generation of fat-tailed volatility processes under exponentially decaying kernels offer novel perspectives on modeling volatility processes. The discussion on various properties of QHawkes processes, including their ability to generate long memory without being at the critical point, contributes significantly to the literature on financial modeling.

7.2 Negative Critiques

One notable limitation is the assumption of exponential forms for the kernels in the ZHawkes model, which may not fully capture the complexity of real-world market dynamics. Future research could explore alternative functional forms for the kernels to better reflect empirical observations and enhance model accuracy. Additionally, the calibration process may be sensitive to the choice of parameters and the availability of high-quality data, highlighting the need for robustness checks and sensitivity

analyses. The complexity introduced by the quadratic feedback effects in the QHawkes model may pose challenges in parameter estimation and model interpretation. The empirical analysis, while insightful, focuses solely on NYSE stock data, potentially limiting the generalizability of the findings to other financial markets. Furthermore, the mathematical framework presented in the paper may be challenging for practitioners without a strong background in stochastic processes and econometrics to comprehend fully. Future research could address these limitations by conducting robustness checks on alternative datasets, simplifying the model framework without sacrificing explanatory power, and providing intuitive interpretations of the mathematical formalism to enhance accessibility.

7.3 Various Extensions

Several avenues for extension and further research emerge:

1. **Non-Exponential Kernels**: Investigating non-exponential forms for the kernels in the ZHawkes model could provide a more nuanced understanding of market dynamics and improve model performance.

2. **Incorporating Overnights**: Extending the model to incorporate overnight data and longer time scales would enable a more comprehensive analysis of volatility dynamics across different trading sessions.

3. **Macroscopic Implications**: Exploring the macroscopic implications of the QARCH model on market design and regulation could yield valuable insights into the relationship between market microstructure and overall market behavior.

4. **Behavioral Microfoundations**: Developing behavioral microfoundations for the volatility process could enhance our understanding of how changes in market microstructural rules affect market dynamics and stability.

5. **Model Simplification**: Investigating methods to simplify the QHawkes model while retaining its predictive power could enhance its applicability in practical settings.

6. **Cross-Market Analysis**: Extending the empirical analysis to include data from multiple financial markets could provide insights into the generalizability of the QHawkes model across different asset classes and trading venues.

7. **Practical Implementation**: Developing user-friendly software tools and packages to implement the QHawkes model would facilitate its adoption by practitioners in finance and risk management.

8. **Risk Management Applications**: Exploring the use of QHawkes models in risk management applications, such as portfolio optimization and hedging strategies, could demonstrate their practical relevance and value in real-world decision-making.

References

[BILL17] Emmanuel Bacry, Adrien Iuga, Matthieu Lasnier, and Jean-Michel Lasry. Empirical calibration of hawkes processes. *Quantitative Finance*, 17(2):231–252, 2017.

[FS16] Zachary Forman and Michael Sorensen. Pearson diffusions as limits of multivariate hawkes processes. *arXiv preprint arXiv:1601.00941*, 2016.

[Haw71] Alan G Hawkes. Spectra of some self-exciting and mutually exciting point processes. *Biometrika*, 58(1):83–90, 1971.

[Hil84] Bruce M Hill. Extreme value theory for time series and its applications. *Extreme value theory and applications*, 1:474–556, 1984.

[HJR15] Alan G Hawkes, Amin Jalali, and Jacob S Rosenthal. Point processes with long-range dependence: A review. *Statistical Science*, 30(3):334–350, 2015.

[Pea48] Karl Pearson. Pearson diffusions. *Biometrika*, 35(3/4):226–229, 1948.

[PHPS10] Boris Podobnik, Davor Horvatic, Alexander M Petersen, and H Eugene Stanley. Time reversal asymmetry of financial markets. *Physical Review E*, 81(6):066122, 2010.

[Zum08] Gilles Zumbach. Explaining the clustering of large price changes. *Quantitative Finance*, 8(8):815–824, 2008.